

## A hybrid surface passivation on HgCdTe long wave infrared detector with *in-situ* CdTe deposition and high-density hydrogen plasma modification

W. D. Hu,<sup>1,a)</sup> X. S. Chen,<sup>1,a)</sup> Z. H. Ye,<sup>2</sup> and W. Lu<sup>1,a)</sup>

<sup>1</sup>National Laboratory for Infrared Physics, Shanghai Institute of Technical Physics, Chinese Academy of Sciences, Shanghai 200083, China

<sup>2</sup>Key Laboratory of Infrared Imaging Materials and Detectors, Shanghai Institute of Technical Physics, Chinese Academy of Sciences, Shanghai 200083, China

(Received 6 June 2011; accepted 12 August 2011; published online 29 August 2011)

A hybrid surface passivation, *in-situ* CdTe passivation and high-density hydrogen plasma modification, is used to improve the surface quality of typical n<sup>+</sup>-on-p HgCdTe long wave infrared photodiode detectors. Three types of surface-passivated pixels, conventional, *in-situ* CdTe, and hybrid surface passivation, are fabricated in one chip for better comparison. The maximum dynamic resistances of the hybrid-surface-passivation device are increased to 1~2 times greater than that in the conventional surface passivation technique. Theoretical modeling shows that the hybrid passivation can significantly suppress the trap-assisted tunneling current. Shallow traps close to the Fermi level under reverse voltage, which are the main source of the trap-assisted tunneling current for conventional surface passivation processing, are reduced by the hybrid passivation treatment. © 2011 American Institute of Physics. [doi:10.1063/1.3633103]

Detection in the long wave infrared range (LWIR, 8–12  $\mu\text{m}$ ) using third generation infrared focal plane array (FPAs), is essential for remote atmosphere sounding. Indeed, these wavelengths, including the very long wave infrared range, VLWIR, ( $\sim 14 \mu\text{m}$ ) are particularly rich in information about humidity and CO<sub>2</sub> levels and provide additional information about cloud structure and temperature profile across the atmosphere.<sup>1–4</sup> However, the dark current characteristic and associated noise behavior of the HgCdTe photodiode in the wavelength range of 8–12  $\mu\text{m}$ , operating at  $\sim 77 \text{ K}$ , are very sensitive to surface passivation techniques as well as to surface material treatments.<sup>5</sup> For current HgCdTe material and device technology, detection of LWIR and VLWIR energy is the subject of current research. Within this range of shrinking band-gaps in detector material, precise control of the quality of the surface passivation and treatment is of great importance.<sup>6–8</sup>

Because of being fabricated on the same chip, the different units have better comparability with each other. In this paper, many special n<sup>+</sup>-on-p HgCdTe detector units have been fabricated on the same chip via three different types of surface passivation techniques: the conventional standard technique, *in-situ* CdTe surface passivation, and hybrid surface passivation (a hybrid of *in-situ* CdTe passivation and high-density hydrogen plasma modification). The maximum dynamic resistances of the hybrid-surface-passivation device are increased to 1~2 times than that of conventional standard surface passivation technique. In addition, the underlying physics of surface trap-related dark current mechanism is theoretically investigated by using a previously developed simultaneous current extraction approach.<sup>3,8</sup>

The HgCdTe films used in the experiment were grown on a semi-insulating GaAs substrate of (211) B orientation with a Riber 32P MBE system.<sup>9,10</sup> The p-type material was achieved by a post-growth p-annealing process with a doping density of  $1.06 \times 10^{16} \text{ cm}^{-3}$ . The cadmium composition  $x$  in the HgCdTe epilayer is 0.22. At the end of MBE material growth, a 2000 Å CdTe dielectric film was *in situ* grown over the HgCdTe surface. The junction area is  $30 \times 30 \mu\text{m}^2$ , B<sup>+</sup> implantation window is defined as  $22 \times 22 \mu\text{m}^2$ , and metallization window is defined as  $8 \times 8 \mu\text{m}^2$ .

Figure 1 shows the process flow chart of the hybrid surface passivation for the n<sup>+</sup>-on-p LWIR HgCdTe detector arrays. Details of the conventional standard techniques can be found in elsewhere.<sup>3,11,12</sup> The *in-situ* CdTe surface passivation technique refers to the process flow of the hybrid surface passivation without the high-density hydrogen plasma modification. The main improvements of the hybrid technique are: (1) the *in situ* deposited CdTe is not entirely removed and HgCdTe surface remains unexposed to the air during the device fabrication; and (2) a low energy hydrogen plasma is used to modify the damage after the B<sup>+</sup> implantation step with inductively coupled plasma (ICP) enhanced RIE instrument. All etch experiments of HgCdTe material masked with photoresist or ZnS film patterns were carried out by applying the optimized process achieved from the photoresist mask technique formerly in the OXFORD ICP 80 instrument.<sup>13,14</sup>

The measured dynamic resistance and dark current values as a function of the different surface passivation techniques are shown in Fig. 2. The maximum dynamic resistances with *in-situ* CdTe passivation are improved more than 100% greater than those produced with the common technique. It is shown that a favorable improvement of the dynamic resistances (about 2 times greater than those with the common technique) is obtained with the hybrid passivation process. To reveal the dark current limiting mechanisms for the different passivation techniques, a sophisticated simultaneous-mode *I-V*

<sup>a)</sup>Authors to whom correspondence should be addressed. Electronic address: wdhu@mail.sitp.ac.cn, xschen@mail.sitp.ac.cn and luwei@mail.sitp.ac.cn.

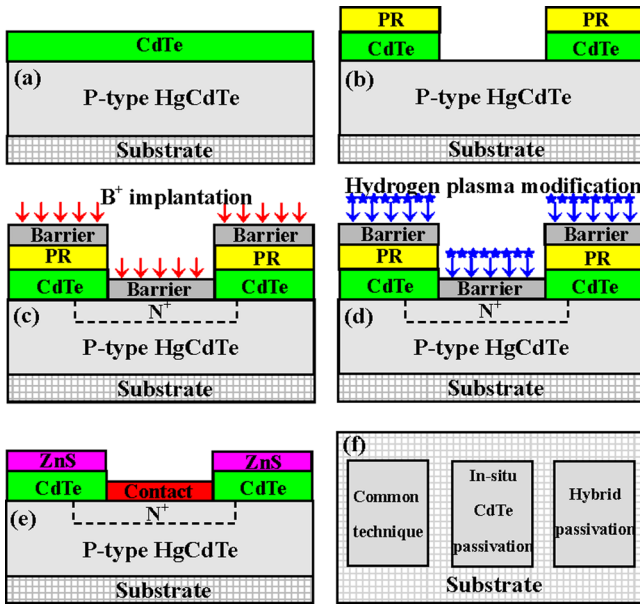


FIG. 1. (Color online) Process flow chart of hybrid surface passivation for  $n^+$ -on-p HgCdTe long wave detector arrays. (a) covering the thin layer of CdTe dielectric film on rinsed HgCdTe epitaxial film; (b) defining the implantation-window patterns with photolithography and exposing HgCdTe surface as implantation-window patterns after selectively etching CdTe film; (c) depositing ZnS film as implantation barrier layers and implanting  $B^+$  into implantation-window patterns to form  $n^+$ -on-p photodiode arrays; (d) low energy hydrogen plasma modification of photodiodes; (e) removing the barrier layer and photoresist and depositing ZnS film to cover the surface of photodiode arrays to form double-layer passivation, then exposing HgCdTe surface as metallization patterns with selective etching ZnS film and depositing the metallization electrode; (f) fabricated three type surface-passivated pixels in one same chip.

fitting program<sup>3</sup> has been used. Two characteristic parameters, the characteristic trap levels and the density of the trap level in the depletion region, are extracted from the measured  $R$ - $V$ s of the different passivation techniques. Other input parameters, such as minority lifetimes, dopant density in the n-region, and series resistance, are selected as known input values from specific experimental measurements. Those input parameters are maintained at the same value during the theoretical modeling as in the three types of surface-passivated pixels fabricated in one chip by the same processes.

Tunneling via SRH centers located within the bandgap dominates under sufficiently high reverse bias and at low-temperatures. This trap-assisted tunneling (TAT) current,  $I_{\text{tat}}$ , can be written as:<sup>3,11</sup>

$$I_{\text{tat}} = -A \cdot \frac{\pi^2 q^2 N_t m_e^* M^2 (V_{\text{bi}} - V_d)}{h^3 (E_g - E_t)} \exp\left(-\frac{\sqrt{3} E_g^2 F(a)}{8\sqrt{2} q P E}\right), \quad (1)$$

$$F(a) = \frac{\pi}{2} + \sin^{-1}(1 - 2a) + 2(1 - 2a)\sqrt{a(1 - a)},$$

$$a = E_t/E_g, \quad (2)$$

where  $E_g$  is the bandgap energy,  $m_e^*$  is the electron effective mass,  $P$  is the Kane matrix element,  $M$  is the transition matrix element between the trap level and conduction band,  $N_t$  is the density of traps in the bulk, and all other symbols have their usual meaning.

The dynamic resistance for different dark current mechanisms is defined as  $R_{\text{diff}} = (dI_{\text{diff}}/dV_e)^{-1}$ ,  $R_{\text{gr}} = (dI_{\text{gr}}/dV_e)^{-1}$ ,  $R_{\text{tat}} = (dI_{\text{tat}}/dV_e)^{-1}$ , and  $R_{\text{bbt}} = (dI_{\text{bbt}}/dV_e)^{-1}$  for the  $I_{\text{diff}}$ -related,  $I_{\text{gr}}$ -related,  $I_{\text{tat}}$ -related, and  $I_{\text{bbt}}$ -related dynamic resistances, respectively.  $I_{\text{diff}}$ ,  $I_{\text{gr}}$ ,  $I_{\text{tat}}$ , and  $I_{\text{bbt}}$  are the diffusion current, generation-recombination current, trap-assisted tunneling current, and band-to-band tunneling current. The total dynamic resistance is given as

$$R_{\text{fit}} = (1/R_{\text{diff}} + 1/R_{\text{gr}} + 1/R_{\text{tat}} + 1/R_{\text{bbt}})^{-1} + R_s, \quad (3)$$

where  $R_s$  is the series resistance. A theoretical  $R$ - $V$  curve can be obtained from substituting a set of the input parameters and fitting parameters into Eq. (3). In our fitting procedure, the algorithm is to minimize the function value of  $F = \sum_{i=1}^N [\log(R_{\text{fit}}(V_{\text{di}})) - \log(R_{\text{exp}}(V_{\text{di}}))]^2$ . There are two fitting parameters to be extracted from  $R$ - $V$  curves for planar  $n$ -on-p MCT photodiodes as follows: the relative energy position of trap level  $E_t/E_g$  and its density  $N_t$  in the depletion region. The detailed modeling procedure can be found in Refs. 3 and 8.

Table I shows the extracted characteristic parameters corresponding to trap-assisted current components by using the simultaneous current extracting approach. Results of this approach show that the extracted characteristic parameters are decreased by using the *in-situ* CdTe passivation and hybrid passivation, as shown in Fig. 3. The shallow trap-levels are changed to the deep trap-levels due to the *in-situ* CdTe passivation. Note that the hybrid passivation does not make a significant contribution to trap-levels. It means that the *in-situ* CdTe passivation can significantly eliminate the shallow trap-levels, which can induce the trap-assisted current. However, hybrid passivation decreases trap densities

TABLE I. Extracted characteristic parameters corresponding to trap-assisted current components by using developed simultaneous current extracting approach.

	$E_t/E_g$	$N_t$ ( $\text{cm}^{-3}$ )
Common technique	0.74	$6.24 \times 10^{12}$
<i>In-situ</i> CdTe passivation	0.52	$2.36 \times 10^{12}$
	0.53	$2.64 \times 10^{12}$
Hybrid passivation	0.52	$1.52 \times 10^{12}$
	0.54	$2.10 \times 10^{12}$

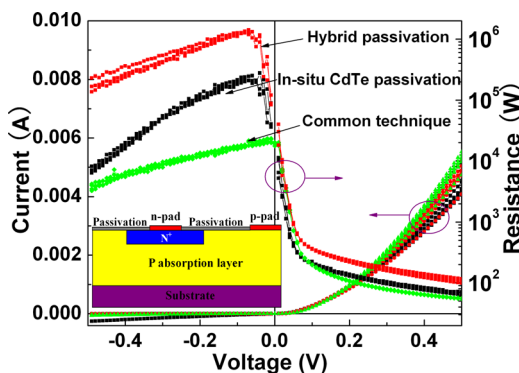


FIG. 2. (Color online) Measured dynamic resistance (right axis) and dark current (left axis) with different surface passivation techniques.

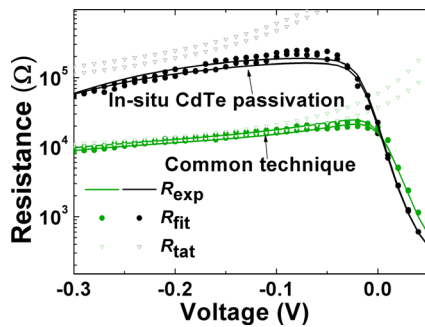


FIG. 3. (Color online) Measured  $R$ - $V$  curves and fitted trap-assisted current components for the conventional technique and *in-situ* CdTe passivation. The data with hybrid surface passivation are not list in the figure for better view of extracted current components.  $R_{\text{exp}}$ (dotted) is the experimental data of total dynamic resistance,  $R_{\text{fit}}$ (dotted) is the fitting data of total dynamic resistance, and  $R_{\text{tat}}$ (triangular) is the dynamic resistance of trap assisted tunneling current.

because the high-density hydrogen plasma modification can passivate the structural defects, such as threading or misfit dislocations, and processing damage, such as plasma damage or thermal damage, that exist in the surface of HgCdTe and CdTe layers due to the still immature of CdTe passivation technology. So, one can conclude that the *in-situ* CdTe passivation and hybrid passivation are beneficial to suppress the trap-assisted tunneling currents of the HgCdTe LWIR detector photodiodes, especially the hybrid passivation. This will enhance the operating dynamic range and performance uniformity, thus improve the property of the HgCdTe long wave photodiodes.

In summary, a hybrid surface passivation, consisting of *in-situ* CdTe passivation and high-density hydrogen plasma modification, is used to improve surface quality of typical  $n^+$ -on- $p$  HgCdTe LWIR photodiode. It is found that the hybrid passivation is beneficial to suppress the trap-assisted tunneling currents of the HgCdTe LWIR photodiodes. The maximum dynamic resistances with hybrid passivation are improved by about a factor of 2 times greater than with the common technique. A sophisticated simultaneous-mode  $I$ - $V$

fitting program has been used to reveal the dark current limiting mechanisms for the different passivation techniques. *In-situ* CdTe passivation can significantly eliminate the shallow trap-levels, which can induce the trap-assisted tunneling process. Hybrid passivation decreases the trap densities, which is the main source of the trap-assisted tunneling current, because the high-density hydrogen plasma modification can passivate many structural defects.

This work was supported in part by the National Natural Science Foundation of China (61006090, 10725418, 10734090, 10990104, 60976092, 61006091, and 60811120169), Key Fund of Shanghai Science and Technology Foundation (09DJ1400203 and 10JC1416100), and International Collaboration Project of Shanghai Science and Technology Foundation (10510704700).

- <sup>1</sup>A. Rogalski, J. Antoszewski, and L. Faraone, *J. Appl. Phys.* **105**, 091101 (2009).
- <sup>2</sup>M. A. Kinch, C. F. Wan, H. Schaaek, and D. Chandra, *Appl. Phys. Lett.* **94**, 193508 (2009).
- <sup>3</sup>W. D. Hu, X. S. Chen, F. Yin, Z. J. Quan, Z. H. Ye, X. N. Hu, Z. F. Li, and W. Lu, *J. Appl. Phys.* **105**, 104502 (2009).
- <sup>4</sup>P. Norton, *Opto-Electron. Rev.* **10**, 159 (2002).
- <sup>5</sup>M. Y. Lee, Y. S. Lee, and H. C. Lee, *Jpn. J. Appl. Phys.*, Part 2 **44**, L1252 (2005).
- <sup>6</sup>M. Y. Lee, Y. S. Lee, and H. C. Lee, *Appl. Phys. Lett.* **88**, 204101 (2006).
- <sup>7</sup>A. Jozwikowska, K. Jozwikowski, J. Antoszewski, C. A. Musca, T. Nguyen, R. H. Sewell, J. M. Dell, L. Faraone, and Z. Orman, *J. Appl. Phys.* **98**, 014504 (2005).
- <sup>8</sup>Z. J. Quan, Z. F. Li, W. D. Hu, Z. H. Ye, X. N. Hu, and W. Lu, *J. Appl. Phys.* **100**, 084503 (2006).
- <sup>9</sup>J. Shao, L. Chen, W. Lü, X. Lü, L. Q. Zhu, S. L. Guo, L. He, and J. H. Chu, *Appl. Phys. Lett.* **96**, 121915 (2010).
- <sup>10</sup>G. K. O. Tsen, C. A. Musca, J. M. Dell, J. Antoszewski, L. Faraone, and C. R. Becker, *Appl. Phys. Lett.* **92**, 082107 (2008).
- <sup>11</sup>G. B. Chen, W. Lu, X. S. Chen, Z. F. Li, W. Y. Cai, L. He, X. N. Hu, and S. C. Shen, *Semicond. Sci. Technol.* **18**, 887 (2003).
- <sup>12</sup>Y. H. Kim, S. H. Bae, H. C. Lee, and C. K. Kim, *J. Electron. Mater.* **29**, 832 (2000).
- <sup>13</sup>W. D. Hu, X. S. Chen, Z. H. Ye, and W. Lu, *Semicond. Sci. Technol.* **25**, 045028 (2010).
- <sup>14</sup>W. D. Hu, X. S. Chen, Z. H. Ye, and W. Lu, *J. Electron. Mater.* **39**, 981 (2010).